JACS
JOURNAL OF THE AMERICAN CHEMICAL SOCIETY

Article

pubs.acs.org/JACS

"Conformation Locked" Strong Electron-Deficient Poly(*p*-Phenylene Vinylene) Derivatives for Ambient-Stable n-Type Field-Effect Transistors: Synthesis, Properties, and Effects of Fluorine Substitution Position

Ting Lei,[†] Xin Xia,[‡] Jie-Yu Wang,[†,*] Chen-Jiang Liu,[‡,*] and Jian Pei[†,*]

[†]Beijing National Laboratory for Molecular Sciences, the Key Laboratory of Bioorganic Chemistry and Molecular Engineering of Ministry of Education, College of Chemistry and Molecular Engineering, Peking University, Beijing 100871, People's Republic of China

[‡]Physics and Chemistry Detecting Center, the Key Laboratory of Oil & Gas Fine Chemicals of Ministry of Education, School of Chemistry and Chemical Engineering, Xinjiang University, Urumqi 830046, People's Republic of China

Supporting Information

ABSTRACT: The charge carrier mobility of p-type and ambipolar polymer field-effect transistors (FETs) has been improved substantially. Nonetheless, high-mobility n-type polymers are rare, and few can be operated under ambient conditions. This situation is mainly caused by the scarcity of strong electron-deficient building blocks. Herein, we present two novel electron-deficient building blocks, **FBDOPV-1** and **FBDOPV-2**, with low LUMO levels down to −4.38 eV. On the basis of both building blocks, we develop two poly(*p*-phenylene vinylene) derivatives (PPVs), **FBDPPV-1** and **FBDPPV-2**, for high-performance n-type polymer FETs. The introduction of the fluorine atoms effectively lowers the LUMO levels of both polymers, leading to LUMO levels as low as −4.30 eV. Fluorination endows both polymers with not only lower LUMO levels, but also more ordered thin-film packing, smaller $\pi-\pi$ stacking distance, stronger interchain interaction and locked conformation of polymer backbones. All these factors provide **FBDPPV-1** with high electron mobilities up to 1.70 $cm^2 V^{-1} s^{-1}$ and good stability under ambient conditions. Furthermore, when polymers have different fluorination positions, their backbone conformations in solid state differ, eventually leading to different device performance.

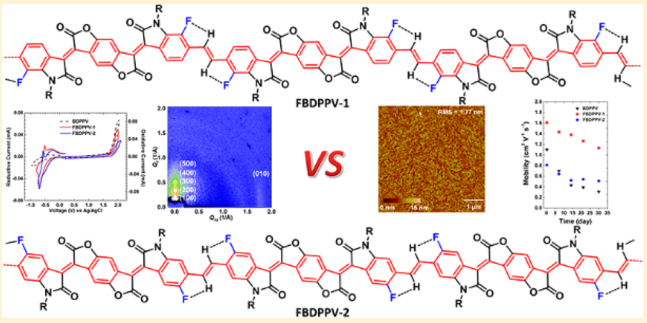

INTRODUCTION

Conjugated polymers are promising active layers for low-cost flexible electronics because their optoelectronic properties can be tuned, and they are solution processable, mechanically flexible, and compatible with heat-sensitive substrates.[1] The development of novel building blocks and fabrication processes have led to significant progress of polymer semiconductors.[2−4] For instance, polymer field-effect transistors (FETs) have been significantly developed due to the design and application of electron-deficient aromatics, such as benzothiadiazole (BT),[5,6] naphthalene diimide (NDI),[7,8] benzobisthiadiazole (BBT),[9,10] diketopyrrolopyrrole (DPP),[3,11−13] and isoindigo (II)[14−17] (Figure 1). High hole mobilities over 10 $cm^2 V^{-1} s^{-1}$ have been achieved for polymer FETs,[12,13] which are comparable with the performance of vacuum-deposited organic thin-film transistors and many organic single-crystal transistors.[18] Compared to many high-mobility p-type polymers, high-mobility n-type polymers are rare, and few can be operated under ambient conditions.[8,19−22] Developing ambient-stable n-type semiconductors becomes a critical issue in organic electronics, because both n-type and p-type semiconductors are necessary to achieve low power complementary circuits.[23]

To date, the development of strong electron-deficient building blocks remains essential to advancing n-type polymer semiconductors.[18,19] Introducing electron-withdrawing groups can effectively lower the lowest unoccupied molecular orbital (LUMO) level of a known building block.[24,25] For example, fluorination of polymer backbones can improve the performance of organic photovoltaics[26,27] and increase the electron mobility of ambipolar polymer FETs.[28,29] Obviously, fluorination can modulate the energy-level of conjugated polymers; nonetheless, it must have other influences on polymer properties, which are important yet seldom investigated.

Charge transport in conjugated polymer films generally contains intrachain and interchain transport. The intrachain mobility of conjugated polymers can be very high.[30] Reducing torsional angles or using shape-persistent backbones will enhance intrachain transport through increasing effective

Received: December 10, 2013
Published: January 15, 2014

   dx.doi.org/10.1021/ja412533d | *J. Am. Chem. Soc.* 2014, 136, 2135−2141

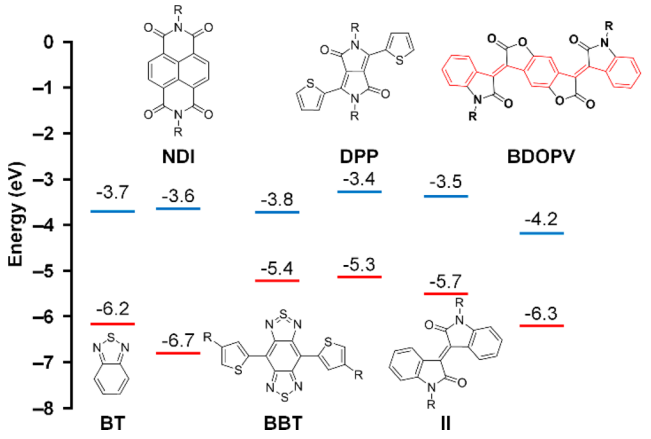

Figure 1. Chemical structures and HOMO/LUMO levels of several electron-deficient building blocks used for high-performance polymer FETs.[4]

conjugation length.[30] For interchain transport, shape-persistent polymer backbones and well-ordered backbone conformations are anticipated because they could provide better $\pi-\pi$ interactions and ordered polymer packing.[31] Recently, benzodifurandione-based oligo(*p*-phenylene vinylene) (**BDOPV**) was developed for ambipolar and n-type polymer FETs (Figure 1).[32−34] **BDOPV** is an electron-deficient building block, which can be regarded as a derivative of oligo(*p*-phenylene vinylene) (OPV). It has four electron-withdrawing carbonyl groups and a low LUMO level of −4.24 eV, significantly lower than those of many electron-deficient building blocks (Figure 1). In addition, these carbonyl groups form four intramolecular hydrogen bonds with the neighboring phenyl protons, making **BDOPV** planar and shape-persistent. Using **BDOPV** as building block, we prepared benzodifurandione-based poly(*p*-phenylene vinylene) (**BDPPV**) (Figure 2).[32] This polymer has high electron mobilities up to 1.1 cm^2 V^{-1} s^{-1}, because it overcomes common defects in poly(*p*-phenylene vinylene) derivatives (PPVs), such as conformational disorder (freely rotating double-bonds), weak interchain interaction, and high LUMO level.[32] Nonetheless, only two-third of the double bonds in this polymer are "locked" by intramolecular hydrogen bonds, thus the polymer backbone still undergoes conformational disorder in solid state. Moreover, although this polymer exhibited outstanding stability in n-type polymer FETs, its device performance still deteriorates under ambient conditions.

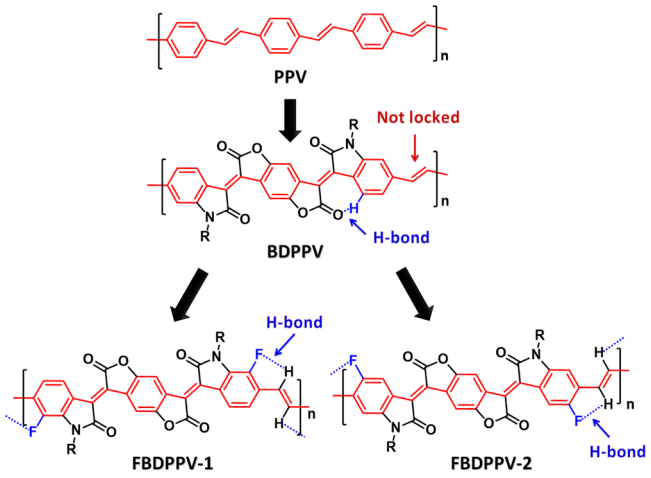

Figure 2. Design strategy of fully "conformation locked" PPV-based conjugated polymers, **FBDPPV-1** and **FBDPPV-2**.

Herein, we attempt to "lock" the remaining one-third of the double bonds in **BDPPV** by introducing fluorine atoms to form more intramolecular hydrogen bonds (Figure 2). We first synthesized two new building blocks, **FBDOPV-1** and **FBDOPV-2**, with fluorine atoms at different positions of **BDOPV**. Both of them have perhaps the lowest LUMO levels (down to −4.38 eV) in polymer building blocks reported to date. Then they were used to prepare two new PPV derivatives, **FBDPPV-1** and **FBDPPV-2** (Figure 2).[18] Fluorine atoms can lower the LUMO levels and fully "lock" the conformations of polymer backbones through intramolecular hydrogen bonds. High-performance n-type FETs based on these two polymers were fabricated. To our delight, **FBDPPV-1** exhibits electron mobilities up to 1.70 cm^2 V^{-1} s^{-1} under ambient conditions, which is among the highest in n-type conjugated polymers and is also a new record for ambient-stable n-type polymer FETs.[8,18,19] Both polymers have improved stability under ambient conditions due to their low-lying LUMO levels. In addition, when the fluorine atoms are substituted in different positions of the polymer backbone, different conformations are created, which eventually leads to different device performance.

RESULTS AND DISCUSSION

Design Strategy and Synthesis. Construction of donor−acceptor polymers can achieve high carrier mobilities.[1,4] Nonetheless, we did not use this strategy in the design of a "pure" n-type transporting system, because this strategy usually increases the highest occupied molecular orbital (HOMO) levels of conjugated polymers, resulting in hole injection, low on/off ratio, or ambipolar transport.[33,34] Moreover, electron-rich donors also increase the LUMO levels of conjugated polymers, thus making the electron transport more susceptible to oxygen and moisture.[35] Alternatively, a double bond was used to link the **BDOPV** units due to its weak electron-donating property. Furthermore, we and other groups have demonstrated that carrier mobilities of conjugated polymers could be significantly increased by using farther branched alkyl chains.[11,15,36,37] Thus, long and farther branched 4-octadecyldocosyl groups were used as polymer side chains to guarantee both better interchain interactions and good solubility. To understand how fluorination influences the conjugated polymers, we prepared two similar polymers with different fluorinated positions (Figure 2).

Scheme 1 illustrates the synthetic route to **FBDPPV-1** and **FBDPPV-2**. The synthesis of fluorinated **BDOPV** started from the construction of fluorinated 6-bromoisatin. 6-Bromo-7-fluoroisatin (**1**) was synthesized according to our previous report.[29] 6-Bromo-5-fluoroisatin (**7**) was synthesized from commercially available 3-bromo-4-fluoroaniline by the condensation reaction of chloral hydrate and hydroxylamine hydrochloride, followed by catalyzed cyclization using sulfuric acid. Both fluorinated isatins (**1** and **7**) were then alkylated with 19-(3-iodopropyl)heptatriacontane (**2**) in the presence of K_2CO_3, and both compounds **3** and **8** were obtained in good yields. **FBDOPV-1** or **FBDOPV-2** were readily obtained with 67% or 78% yield by using a simple acidic condensation condition between **3** or **8** and 2,2′-(2,5-dihydroxy-1,4-phenylene)diacetic acid (**9**), respectively.[33] Microwave-assisted Stille coupling polymerizations using (*E*)-1,2-bis-

dx.doi.org/10.1021/ja412533d | J. Am. Chem. Soc. 2014, 136, 2135−2141

Scheme 1. Synthetic Route to Fluorinated BDOPV Derivatives and Fluorinated BDPPV Polymers

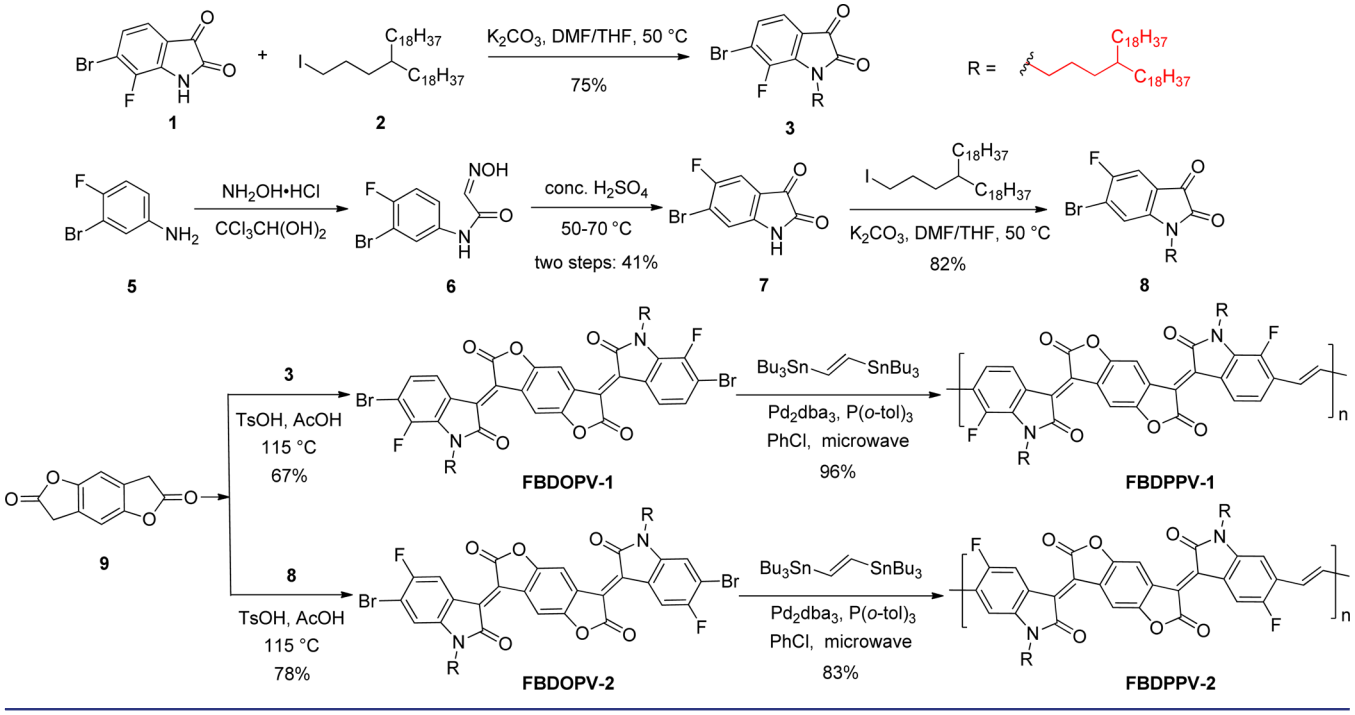

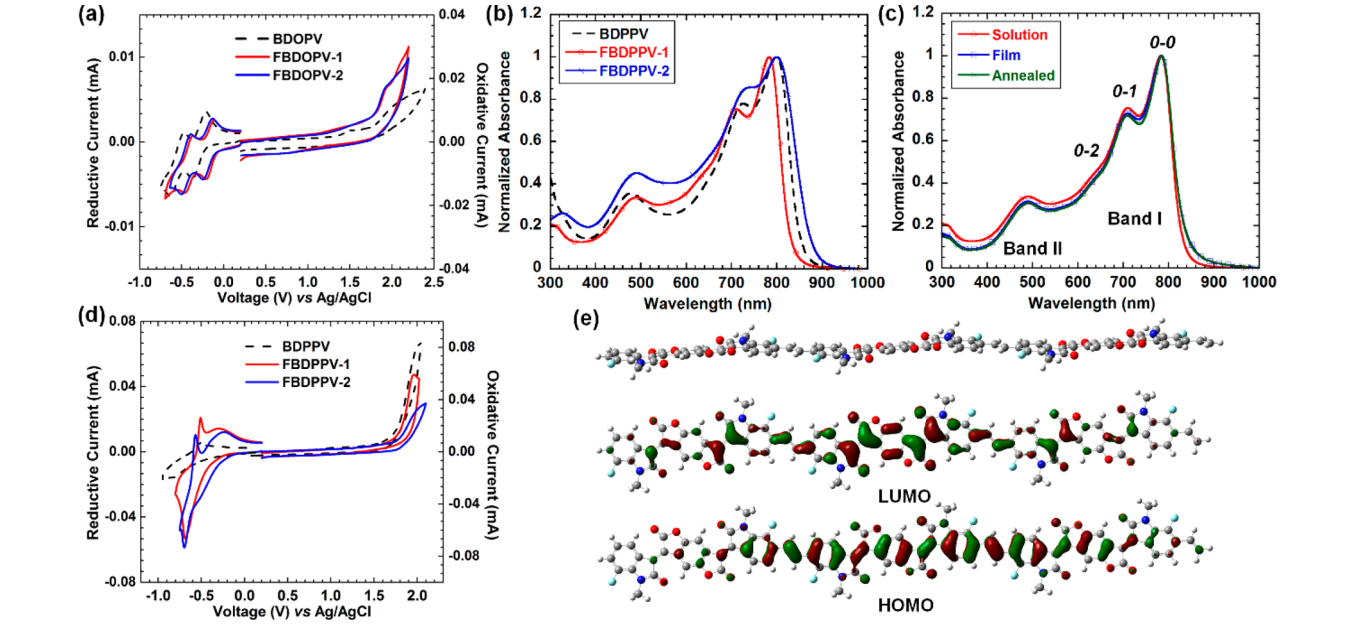

Figure 3. (a) Cyclic voltammograms of **BDOPV** (with bromine), **FBDOPV-1** and **FBDOPV-2** in 1,2-dichlorobenzene (DCB) solution (5 mg/mL). (b) Normalized absorption spectra of three polymers in $CHCl_3$ (10^{-5} M). (c) Normalized absorption spectra of **FBDPPV-1** in $CHCl_3$ (10^{-5} M), thin film and annealed film (180 °C for 30 min). (d) Cyclic voltammograms of three polymers in drop-casted film prepared using their chloroform solutions (5 mg/mL). (e) Molecular frontier orbitals of the **FBDPPV-1** trimer (B3LYP/6-311G(d,p)).

(tributylstannyl)ethene gave polymers **FBDPPV-1** and **FBDPPV-2** in 96% and 83% yield, respectively. The molecular weights of both polymers were evaluated by high-temperature (GPC) at 140 °C using 1,2,4-tricholorobenzene (TCB) as eluent. Both polymers displayed comparable molecular weights (**FBDPPV-1**: M_w = 128.9 kDa, M_n = 66.3 kDa, PDI = 1.94; **FBDPPV-2**: M_w = 164.7 kDa, M_n = 53.8 kDa, PDI = 3.06) (Figure S1 in the Supporting Information, SI) and showed excellent thermal stability with decomposition temperatures over 370 °C (Figure S2 in the SI).

Photophysical and Electrochemical Properties. The aborption sprectra of **FBDOPV-1** and **FBDOPV-2** are smimilar to that of **BDOPV** (with bromine on the same position as **FBDOPV**) due to their identical conjugated backbones (Figure S3 in the SI). After introducing fluorine atoms, both the HOMO and LUMO energy levels of **FBDOPV-1** and **FBDOPV-2** are lowered. The LUMO energy levels are lowered by 0.14 and 0.12 eV for **FBDOPV-1** and **FBDOPV-2**, respectively (Table S1 in the SI). The LUMO level of **FBDOPV-1** reaches −4.38 eV, suggesting that

dx.doi.org/10.1021/ja412533d | J. Am. Chem. Soc. 2014, 136, 2135−2141

Table 1. Summary of Optical and Electrochemical Properties, OFET Device Performance and GIXD Results of Three Polymers

compounds	λ_{max}^{sol} (nm)[a]	λ_{max}^{film} (nm)	E_g (eV)[b]	E_{HOMO} (eV)[c]	E_{LUMO} (eV)[c]	μ (cm^2 V^{-1} s^{-1})[d]	V_T (V)	log (I_{on}/I_{off})	d (Å)[e]	
									L	π
BDPPV	799, 728	803, 724	1.42	−6.12	−4.10	1.10 (0.84)	+5	5−6	32.3	3.45
FBDPPV-1	786, 710	784, 710	1.46	−6.19	−4.26	1.70 (1.39)	+18	5−6	32.9	3.42
FBDPPV-2	800, 740	808, 743	1.39	−6.22	−4.30	0.81 (0.62)	+1	4−5	32.7	3.42

[a] 10^{-5} M in chloroform. [b] Estimated from the onset of the absorption spectra of thin film. [c] Cyclic voltammetry determined with Fc/Fc^+ (E_{HOMO} = −4.80 eV) as external reference. [d] Maximum values of the electron mobilities. Electron mobilities are measured under ambient conditions (R_H = 50−60%). The average values are in parentheses. [e] Lamellar (L) and π−π stacking (π) distances determined by GIXD experiments.

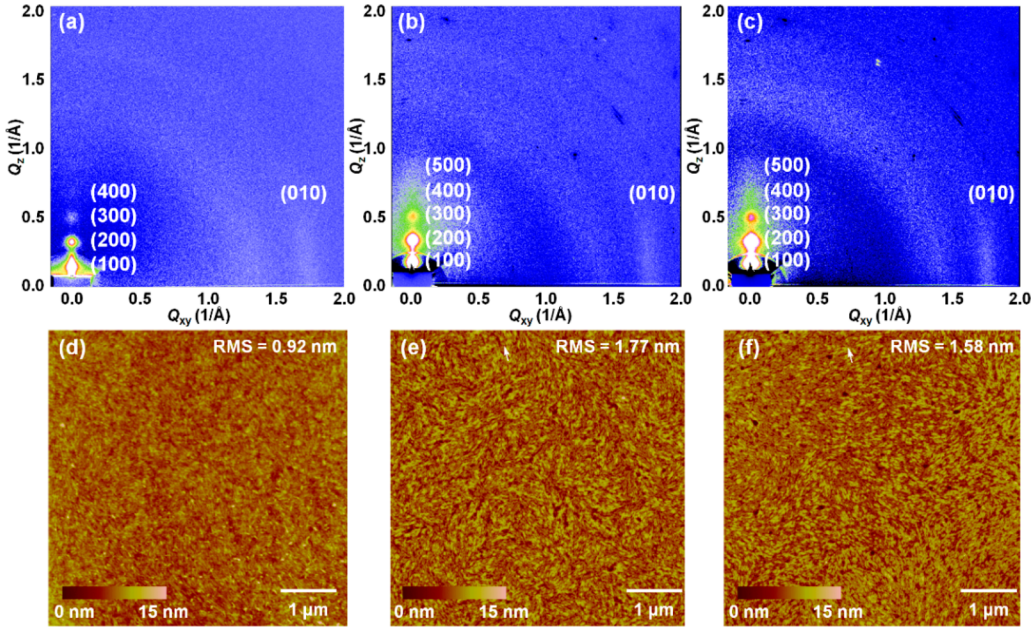

Figure 4. 2D-GIXD patterns and AFM height images of (a, d) **BDPPV**, (b, e) **FBDPPV-1**, and (c, f) **FBDPPV-2** films. Films were prepared by spin-coating their DCB solutions (3 mg/mL) and annealed at 180 °C for 30 min.

FBDOPV-1 is one of the most electron-deficient building blocks for conjugated polymers.[4,38] Note that all three monomers display two reversible reductive peaks in solution (Figure 3a), indicating their good stability in the anionic state.

All these polymers show similar absorption spectra, and all have two absoprtion bands (Band I: 600−900 nm; Band II: 400−600 nm) and low bandgaps around 1.4 eV (Figure 3 and Table 1). All polymers have structured vabrational absorption peaks in the Band I region, which agrees well with their shape-persistent conjugated backbones. Compared with **BDPPV**, **FBDPPV-1** exihbits a blue-shifted absorption spectrum, whereas **FBDPPV-2** exihbits a slightly red-shift. In addtion, three polymers show different oscillator strength of the vabrational absorption peaks. The main absorption peak of **FBDPPV-1** in film only shows very little red-shift compared to that in solution, and an obvious increase of the relative intensity of its *0−0* vibrational peak is observed (Figure 3c). Annealing the film results in a further increase of the relative intensity of *0−0* peak, indicating that the polymer backbone becomes more planar in film and annealing is helpful for further adjustment. For conjugated polymers, intermolecular stacking and conformational change may significantly shift the absorption spectra.[39] However, no significant change was observed from solution to thin film for **FBDPPV-1**, suggesting that the polymer probably formed some preaggregates in solution due to strong interchain interactions.[40,41] Compared with **FBDPPV-1**, **FBDPPV-2** shows a little more red-shifted absorption from solution to film (Figure S4 in the SI), suggesting that both polymers might take different molecular conformations and supramolecular organizations in solid state, although they have very similar conjugated backbones.[39]

Electrochemical properties of three polymers were explored by cyclic voltammetry (CV) measurement (Figure 3d). After introducing fluorine atoms, the reductive currents of both fluorinated polymers increase obviously and the reductive doping processes appear to be more reversible than those of **BDPPV**. Both the HOMO and LUMO energy levels of **FBDPPV-1** and **FBDPPV-2** are lowered, but clearly the LUMO energy levels are more easily affected (Table 1). The LUMO levels of **FBDPPV-1** and **FBDPPV-2** reach −4.26 and −4.30 eV, 0.16 and 0.20 eV lower than that of **BDPPV**. To our knowledge, these polymers are the most electron-deficient conjugated polymers reported to date.[8,19,22,42,43] Computational results reveal that both fluorinated polymers exhibit almost planar conjugated backbones and their HOMOs and LUMOs are well delocalized along polymer backbones (Figure 3e). This contrasts with many donor−acceptor polymers, in which the LUMOs are mostly localized on the electron-deficient cores of polymer backbones.[16,34]

Thin Film Microstructural Characterization. The molecular packings and surface morphologies of three polymer films were invesitgated by grazing incident X-ray diffraction (GIXD) and tapping-mode atomic force microscopy (AFM) (Figure 4). Three polymers display strong out-of-plane

diffractions (h00), indicating that good edge-on lamellar packings are formed in film. Fluorinated polymers show five out-of-plane diffraction peaks, whereas **BDPPV** only shows four out-of-plane peaks. However, three polymers exihbit similar lamellar distances around 32 Å due to their smiliar backbones and identical side chains. (010) Peaks attributed to $\pi-\pi$ stacking were also observed. Clearly, both fluorinated polymers exhibt a stronger (010) peak with a shorter $\pi-\pi$ stacking distance of 3.42 Å, slightly shorter than that of **BDPPV** (3.45 Å). These results suggest that after introducing fluorine atoms, **FBDPPV-1** and **FBDPPV-2** exhibit more ordered lamellar packing and stronger interchain interactions in solid state. This is also supported by the AFM observation that both fluorinated polymers display fiber-like intercalating networks with obviously crystallized zones. Root-mean-square (RMS) analysis of the height data shows that the films of fluorinated polymers display larger roughness, presumably due to their stronger crystallinity. Therefore, the introduction of fluorine atoms not only modulates the energy levels of polymers, but also influences the interchain interactions and polymer packing in solid state.

Field-Effect Transistor Fabrication and Measurements. Top-gate/bottom-contact (TG/BC) device configuration was used to evaluate the carrier transport of both fluorinated polymers (Figure 5a). This device configuration is preferred for many n-type organic materials because of its better injection characteristics and encapsulation effect.[8] The semiconducting layer was deposited by spin-coating a polymer solution (3 mg/mL in DCB) on Au (source-drain)/SiO_2/Si substrate. After thermal annealing, a CYTOP solution was spin-coated on the top of the semiconducting layer and cross-linked under 100 °C for 1 h, providing the dielectric layer (500 nm thick). Then, an aluminum layer was thermally evaporated as the gate electrode. All devices were fabricated in glovebox and tested under ambient conditions (R_H = 50–60%). Both fluorinated polymers show typical n-type transport characteristics under ambient conditions (Figure 5b,d). The maximum mobility of the **FBDPPV-1** devices was determined to be as high as 1.70 $cm^2\ V^{-1}\ s^{-1}$, which is among the highest in n-type conjugated polymers and is also a new record for n-type polymer FETs operated under ambient conditions.[8,19] Note that **FBDPPV-1** shows typical transfer and output characteristics with negligible hysteresis, which is seldom observed for n-type organic materials, largely attributed to its significantly lowered LUMO level. Besides, no contact resistance was observed in output curves, suggesting a good contact between the polymer and gold electrode. However, **FBDPPV-2** only gave the highest electron mobility of 0.81 $cm^2\ V^{-1}\ s^{-1}$ and an average mobility of 0.62 $cm^2\ V^{-1}\ s^{-1}$, unexpectedly lower than that of nonfluorinated **BDPPV** (highest: 1.10 $cm^2\ V^{-1}\ s^{-1}$; average: 0.84 $cm^2\ V^{-1}\ s^{-1}$).

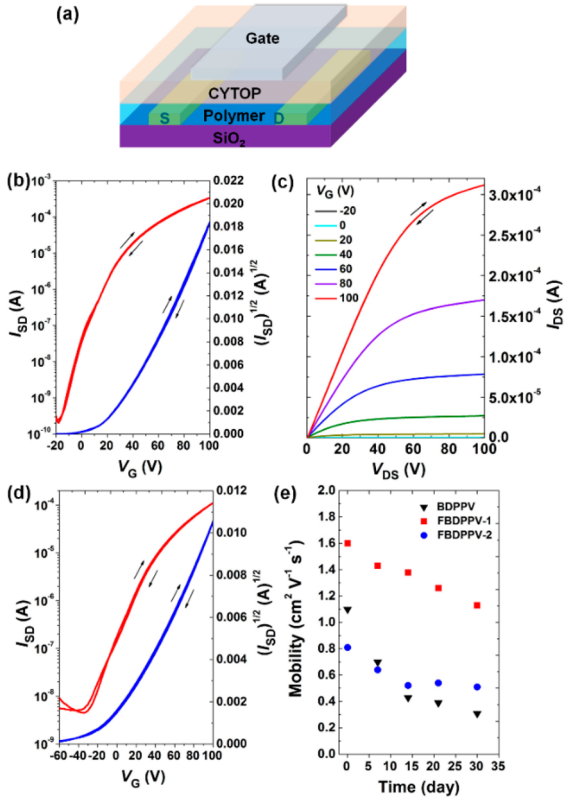

Figure 5. (a) Top-gate/bottom-contact device configuration used in this study. (b) Transfer and (c) output characteristics of a **FBDPPV-1** device measured under ambient conditions. (d) Transfer characteristic of a **FBDPPV-2** device. (e) Time-dependent decays of the device performance of three polymers under ambient conditions. FET devices (L = 5 μm, W = 100 μm,) were fabricated with CYTOP layers around 500 nm thick (capacitance C_i = 3.7 nF cm^{-2}).

Time-dependent decays of three polymer devices were tested by storing the devices under ambient conditions (R_H = 50–60%). All polymers show good stability with a slow roll-off of electron mobility (Figure 5e). Fluorinated polymers show obviously better stability than nonfluorinated **BDPPV**. After 30 days, the mobility of **FBDPPV-1** device decreased from 1.61 to 1.13 $cm^2\ V^{-1}\ s^{-1}$, whereas that of **BDPPV** decreased from 1.10 to 0.31 $cm^2\ V^{-1}\ s^{-1}$. The decay of the electron mobilities may be caused by the further diffusion of oxygen or moisture into the semiconducting layer.[35] Although these devices are not long-term stable under ambient conditions, these results are outstanding among n-type conjugated polymers, because few reported n-type polymers can be operated under ambient conditions.[8,19−22]

Influence of Backbone Conformation on Carrier Mobility. Both fluorinated polymers have considerably different device performance despite their similar physical and electrochemical properties, including molecular weight, thin-film packing, and morphology. We propose that this difference originates from their different polymer backbone conformations in solid state. To give a better understanding, a model compound (E)-1,2-bis(2-fluorophenyl)ethane was used to investigate the double bond conformations of the fluorinated polymers. Figure 6a displays three possible conformations of the model compound. After introducing fluorine atoms, intramolecular hydrogen bonds are formed between fluorine and hydrogen atoms, thus locking the molecular conformation. The five-membered-ring hydrogen bonding is preferred, providing obviously lower energy than the six-membered-ring hydrogen bonding. This computational analysis is supported by single crystal structures of several fluorinated OPV derivatives,[44] in which all of the fluorine atoms formed five-membered-ring hydrogen bonds with neighboring phenyl protons (Figure 6b). These results indicate that both **FBDPPV-1** and **FBDPPV-2** may have "locked" conformations and intramolecular five-membered-ring hydrogen bonds are formed in solid state. Clearly, due to the different substitution position of fluorine, the backbone conformations of both polymers are different. Calculations on the oligomers of

dx.doi.org/10.1021/ja412533d | J. Am. Chem. Soc. 2014, 136, 2135−2141

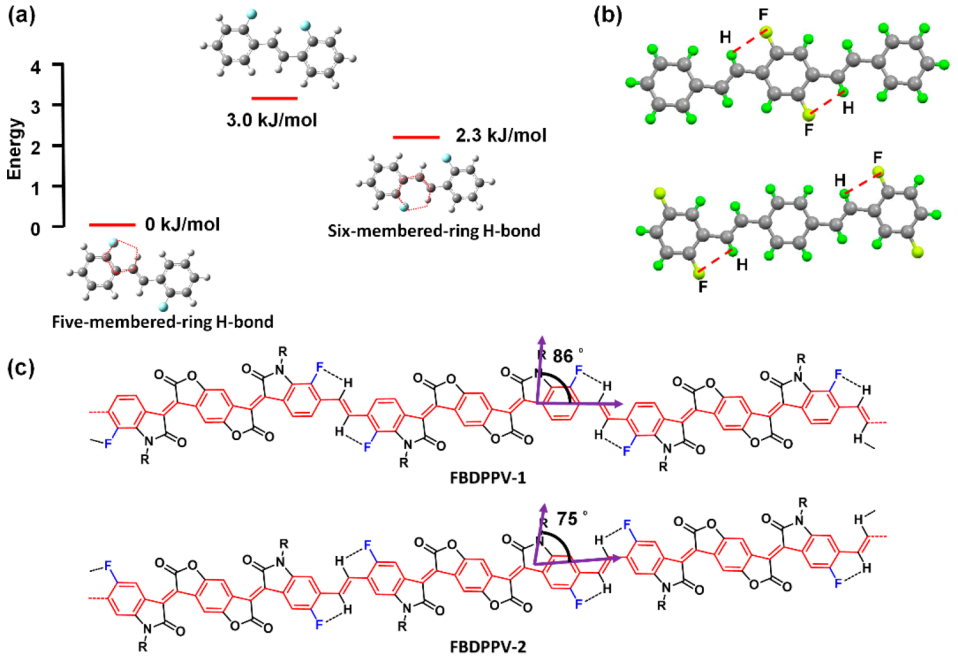

Figure 6. (a) Energy diagram of different planar conformations of model compound (*E*)-1,2-bis(2-fluorophenyl)ethane (calculated at B3LYP/6-311+G(d,p) level). (b) Single crystal structures of two fluorinated OPV derivatives. Both show five-membered-ring intramolecular hydrogen bonds. (c) Proposed intramolecular hydrogen bonds and backbone conformations for **FBDPPV-1** and **FBDPPV-2**.

FBDPPV-1 also show that the five-membered-ring hydrogen-bonding conformation is more stable than other conformations (Figure S7 in the SI).

Using a computational method, Beljonne and co-workers demonstrated that interchain charge transport correlates with the supramolecular organization of conjugated polymers.[45] For example, even under the same $\pi-\pi$ stacking distance, different polymer packing conformations can lead to greatly different interchain carrier transport. This is mainly caused by the different charge transfer integrals between polymer chains.[46] Furthermore, increasing experimental results suggest that polymer backbone conformations indeed exert their influences on carrier transport through adopting various interchain molecular packings.[47,48] Figure 6c shows the proposed intramolecular hydrogen bonds in **FBDPPV-1** and **FBDPPV-2** and their polymer backbone conformations in film. The purple arrows indicate the included angles between the alkyl chain extending directions and the polymer backbone extending directions. Clearly, the double bond orientations are different for both polymers, and the included angle of **FBDPPV-1** is close to 90°, obviously larger than that of **FBDPPV-2**. This analysis agrees with the absorption spectra result that both polymers might have different molecular conformations and supramolecular organization in solid state. Because intermolecular packing and carrier mobility are sensitive to molecular conformations and the orientation of side chains,[46,49,50] the different backbone conformations of **FBDPPV-1** and **FBDPPV-2** might lead to different interchain organization and thereby influence interchain carrier transport. Similarly, due to the ineffective interchain charge transport, **FBDPPV-2** exhibits lower electron mobility than **BDPPV**, even though it has locked conformations, lower LUMO level and stronger crystallinity. However, further investigations are needed to better understand the myriad factors influencing the electron transport of these polymers, but are beyond the scope of this manuscript.

CONCLUSIONS

In conclusion, we have developed two novel strong electron-deficient building blocks, **FBDOPV-1** and **FBDOPV-2**. Both building blocks have extremely low LUMO levels down to −4.38 eV. On the basis of them, two PPV derivatives, **FBDPPV-1** and **FBDPPV-2**, are developed for ambient-stable n-type polymer FETs. Both polymers exhibit improved device stability under ambient conditions due to their low-lying LUMO levels. **FBDPPV-1** has increased electron mobility up to 1.70 $cm^2\ V^{-1}\ s^{-1}$ under ambient conditions, which is among the highest in n-type conjugated polymers, whereas **FBDPPV-2** has decreased electron mobility. Our work demonstrates that fluorination is more than lowering the energy levels of conjugated polymers, it can also influence backbone conformations (hence interchain interactions and film microstructures), which is critical to the device performance. Given the extensive application of fluorination in conjugated polymers, the systematic comparison and conformational consideration presented in this work could provide a new angle to investigate the structure−property relationships of conjugated polymers.

ASSOCIATED CONTENT

Supporting Information

OTFT fabrication details; GPC, TGA, and DSC traces; UV−vis spectra; monomer and polymer synthesis and characterization; and ^1H and ^{13}C NMR spectra. This material is available free of charge via the Internet at http://pubs.acs.org.

AUTHOR INFORMATION

Corresponding Author

jianpei@pku.edu.cn; pxylcj@126.com; jieyuwang@pku.edu.cn

Notes

The authors declare no competing financial interest.

■ ACKNOWLEDGMENTS

This work was supported by the Major State Basic Research Development Program (2013CB933501) from the Ministry of Science and Technology, Urumqi Science and Technology Project (G121120005), and National Natural Science Foundation of China. The authors thank beamline BL14B1 (Shanghai Synchrotron Radiation Facility) for providing the beam time.

■ REFERENCES

(1) Heeger, A. J. *Chem. Soc. Rev.* **2010**, *39*, 2354−2371.
(2) Mei, J.; Diao, Y.; Appleton, A. L.; Fang, L.; Bao, Z. *J. Am. Chem. Soc.* **2013**, *135*, 6724−6746.
(3) Nielsen, C. B.; Turbiez, M.; McCulloch, I. *Adv. Mater.* **2013**, *25*, 1859−1880.
(4) Yuen, J. D.; Wudl, F. *Energy Environ. Sci.* **2013**, *6*, 392−406.
(5) Tsao, H. N.; Cho, D. M.; Park, I.; Hansen, M. R.; Mavrinskiy, A.; Yoon, D. Y.; Graf, R.; Pisula, W.; Spiess, H. W.; Müllen, K. *J. Am. Chem. Soc.* **2011**, *133*, 2605−2612.
(6) Tseng, H.-R.; Ying, L.; Hsu, B. B. Y.; Perez, L. A.; Takacs, C. J.; Bazan, G. C.; Heeger, A. J. *Nano Lett.* **2012**, *12*, 6353−6357.
(7) Zhan, X.; Facchetti, A.; Barlow, S.; Marks, T. J.; Ratner, M. A.; Wasielewski, M. R.; Marder, S. R. *Adv. Mater.* **2011**, *23*, 268−284.
(8) Yan, H.; Chen, Z.; Zheng, Y.; Newman, C.; Quinn, J. R.; Dotz, F.; Kastler, M.; Facchetti, A. *Nature* **2009**, *457*, 679−686.
(9) Fan, J.; Yuen, J. D.; Cui, W.; Seifter, J.; Mohebbi, A. R.; Wang, M.; Zhou, H.; Heeger, A.; Wudl, F. *Adv. Mater.* **2012**, *24*, 6164−6168.
(10) Yuen, J. D.; Fan, J.; Seifter, J.; Lim, B.; Hufschmid, R.; Heeger, A. J.; Wudl, F. *J. Am. Chem. Soc.* **2011**, *133*, 20799−20807.
(11) Lee, J.; Han, A. R.; Yu, H.; Shin, T. J.; Yang, C.; Oh, J. H. *J. Am. Chem. Soc.* **2013**, *135*, 9540−9547.
(12) Kang, I.; Yun, H.-J.; Chung, D. S.; Kwon, S.-K.; Kim, Y.-H. *J. Am. Chem. Soc.* **2013**, *135*, 14896−14899.
(13) Li, J.; Zhao, Y.; Tan, H. S.; Guo, Y.; Di, C.-A.; Yu, G.; Liu, Y.; Lin, M.; Lim, S. H.; Zhou, Y.; Su, H.; Ong, B. S. *Sci. Rep.* **2012**, *2*, 754.
(14) Stalder, R.; Mei, J.; Graham, K. R.; Estrada, L. A.; Reynolds, J. R. *Chem. Mater.* **2014**, *26*, 664−678.
(15) Mei, J.; Kim, D. H.; Ayzner, A. L.; Toney, M. F.; Bao, Z. *J. Am. Chem. Soc.* **2011**, *133*, 20130−20133.
(16) Lei, T.; Cao, Y.; Zhou, X.; Peng, Y.; Bian, J.; Pei, J. *Chem. Mater.* **2012**, *24*, 1762−1770.
(17) Lei, T.; Cao, Y.; Fan, Y.; Liu, C.-J.; Yuan, S.-C.; Pei, J. *J. Am. Chem. Soc.* **2011**, *133*, 6099−6101.
(18) Wang, C.; Dong, H.; Hu, W.; Liu, Y.; Zhu, D. *Chem. Rev.* **2012**, *112*, 2208−2267.
(19) Li, H.; Kim, F. S.; Ren, G.; Jenekhe, S. A. *J. Am. Chem. Soc.* **2013**, *135*, 14920−14923.
(20) Takeda, Y.; Andrew, T. L.; Lobez, J. M.; Mork, A. J.; Swager, T. M. *Angew. Chem., Int. Ed.* **2012**, *51*, 9042−9046.
(21) Lee, J.-K.; Gwinner, M. C.; Berger, R.; Newby, C.; Zentel, R.; Friend, R. H.; Sirringhaus, H.; Ober, C. K. *J. Am. Chem. Soc.* **2011**, *133*, 9949−9951.
(22) Babel, A.; Jenekhe, S. A. *J. Am. Chem. Soc.* **2003**, *125*, 13656−13657.
(23) Zaumseil, J.; Sirringhaus, H. *Chem. Rev.* **2007**, *107*, 1296−1323.
(24) Tang, M. L.; Bao, Z. *Chem. Mater.* **2011**, *23*, 446−455.
(25) Lei, T.; Dou, J.-H.; Ma, Z.-J.; Liu, C.-J.; Wang, J.-Y.; Pei, J. *Chem. Sci.* **2013**, *4*, 2447−2452.
(26) Chen, H.-Y.; Hou, J.; Zhang, S.; Liang, Y.; Yang, G.; Yang, Y.; Yu, L.; Wu, Y.; Li, G. *Nat. Photon.* **2009**, *3*, 649−653.
(27) Bronstein, H.; Frost, J. M.; Hadipour, A.; Kim, Y.; Nielsen, C. B.; Ashraf, R. S.; Rand, B. P.; Watkins, S.; McCulloch, I. *Chem. Mater.* **2013**, *25*, 277−285.
(28) Park, J. H.; Jung, E. H.; Jung, J. W.; Jo, W. H. *Adv. Mater.* **2013**, *25*, 2583−2588.
(29) Lei, T.; Dou, J.-H.; Ma, Z.-J.; Yao, C.-H.; Liu, C.-J.; Wang, J.-Y.; Pei, J. *J. Am. Chem. Soc.* **2012**, *134*, 20025−20028.
(30) Prins, P.; Grozema, F. C.; Schins, J. M.; Patil, S.; Scherf, U.; Siebbeles, L. D. A. *Phys. Rev. Lett.* **2006**, *96*, 146601.
(31) Noriega, R.; Rivnay, J.; Vandewal, K.; Koch, F. P. V.; Stingelin, N.; Smith, P.; Toney, M. F.; Salleo, A. *Nat. Mater.* **2013**, *12*, 1038−1044.
(32) Lei, T.; Dou, J.-H.; Cao, X.-Y.; Wang, J.-Y.; Pei, J. *J. Am. Chem. Soc.* **2013**, *135*, 12168−12171.
(33) Yan, Z.; Sun, B.; Li, Y. *Chem. Commun.* **2013**, *49*, 3790−3792.
(34) Lei, T.; Dou, J. H.; Cao, X. Y.; Wang, J. Y.; Pei, J. *Adv. Mater.* **2013**, *25*, 6589−6593.
(35) Di Pietro, R.; Fazzi, D.; Kehoe, T. B.; Sirringhaus, H. *J. Am. Chem. Soc.* **2012**, *134*, 14877−14889.
(36) Lei, T.; Dou, J.-H.; Pei, J. *Adv. Mater.* **2012**, *24*, 6457−6461.
(37) Zhang, F.; Hu, Y.; Schuettfort, T.; Di, C.-A.; Gao, X.; McNeill, C. R.; Thomsen, L.; Mannsfeld, S. C. B.; Yuan, W.; Sirringhaus, H.; Zhu, D. *J. Am. Chem. Soc.* **2013**, *135*, 2338−2349.
(38) Wen, Y.; Liu, Y.; Guo, Y.; Yu, G.; Hu, W. *Chem. Rev.* **2011**, *111*, 3358−3406.
(39) Kim, J.; Swager, T. M. *Nature* **2001**, *411*, 1030−1034.
(40) Steyrleuthner, R.; Schubert, M.; Howard, I.; Klaumünzer, B.; Schilling, K.; Chen, Z.; Saalfrank, P.; Laquai, F.; Facchetti, A.; Neher, D. *J. Am. Chem. Soc.* **2012**, *134*, 18303−18317.
(41) Zhou, N.; Guo, X.; Ortiz, R. P.; Li, S.; Zhang, S.; Chang, R. P. H.; Facchetti, A.; Marks, T. J. *Adv. Mater.* **2012**, *24*, 2242−2248.
(42) Usta, H.; Newman, C.; Chen, Z.; Facchetti, A. *Adv. Mater.* **2012**, *24*, 3678−3684.
(43) Chen, Z.; Zheng, Y.; Yan, H.; Facchetti, A. *J. Am. Chem. Soc.* **2009**, *131*, 8−9.
(44) Renak, M. L.; Bartholomew, G. P.; Wang, S.; Ricatto, P. J.; Lachicotte, R. J.; Bazan, G. C. *J. Am. Chem. Soc.* **1999**, *121*, 7787−7799.
(45) Niedzialek, D.; Lemaur, V.; Dudenko, D.; Shu, J.; Hansen, M. R.; Andreasen, J. W.; Pisula, W.; Müllen, K.; Cornil, J.; Beljonne, D. *Adv. Mater.* **2013**, *25*, 1939−1947.
(46) Coropceanu, V.; Cornil, J.; da Silva Filho, D. A.; Olivier, Y.; Silbey, R.; Brédas, J.-L. *Chem. Rev.* **2007**, *107*, 926−952.
(47) Osaka, I.; Abe, T.; Shinamura, S.; Takimiya, K. *J. Am. Chem. Soc.* **2011**, *133*, 6852−6860.
(48) Rieger, R.; Beckmann, D.; Mavrinskiy, A.; Kastler, M.; Müllen, K. *Chem. Mater.* **2010**, *22*, 5314−5318.
(49) Lei, T.; Wang, J.-Y.; Pei, J. *Chem. Mater.* **2014**, *26*, 594−603.
(50) Mei, J.; Bao, Z. *Chem. Mater.* **2014**, *26*, 604−615.